# Pak and Rac GTPases promote oncogenic KIT–induced neoplasms

Holly Martin,[1,2] Raghuveer Singh Mali,[2] Peilin Ma,[2] Anindya Chatterjee,[2] Baskar Ramdas,[2] Emily Sims,[2] Veerendra Munugalavadla,[3] Joydeep Ghosh,[2] Ray R. Mattingly,[4] Valeria Visconte,[5] Ramon V. Tiu,[5] Cornelis P. Vlaar,[6] Suranganie Dharmawardhane,[7] and Reuben Kapur[1,2,8]

[1]Department of Medical and Molecular Genetics and [2]Department of Pediatrics, Herman B Wells Center for Pediatric Research, Indiana University School of Medicine, Indianapolis, Indiana, USA. [3]Department of Cancer Immunotherapy and Hematology, Genentech Inc., South San Francisco, California, USA. [4]School of Medicine, Wayne State University, Detroit, Michigan, USA. [5]Department of Translational Hematology and Oncology Research, Taussig Cancer Institute, Cleveland Clinic, Cleveland, Ohio, USA. [6]Department of Pharmaceutical Sciences, School of Pharmacy, and [7]Department of Biochemistry, University of Puerto Rico Medical Sciences Campus, San Juan, Puerto Rico, USA. [8]Department of Molecular Biology and Biochemistry, Indiana University School of Medicine, Indianapolis, Indiana, USA.

**An acquired somatic mutation at codon 816 in the KIT receptor tyrosine kinase is associated with poor prognosis in patients with systemic mastocytosis and acute myeloid leukemia (AML). Treatment of leukemic cells bearing this mutation with an allosteric inhibitor of p21–activated kinase (Pak) or its genetic inactivation results in growth repression due to enhanced apoptosis. Inhibition of the upstream effector Rac abrogates the oncogene-induced growth and activity of Pak. Although both Rac1 and Rac2 are constitutively activated via the guanine nucleotide exchange factor (GEF) Vav1, loss of Rac1 or Rac2 alone moderately corrected the growth of KIT-bearing leukemic cells, whereas the combined loss resulted in 75% growth repression. In vivo, the inhibition of Vav or Rac or Pak delayed the onset of myeloproliferative neoplasms (MPNs) and corrected the associated pathology in mice. To assess the role of Rac GEFs in oncogene-induced transformation, we used an inhibitor of Rac, EHop-016, which specifically targets Vav1 and found that EHop-016 was a potent inhibitor of human and murine leukemic cell growth. These studies identify Pak and Rac GTPases, including Vav1, as potential therapeutic targets in MPN and AML involving an oncogenic form of KIT.**

## Introduction

Gain-of-function mutations in the KIT receptor tyrosine kinase are associated with highly malignant human neoplasms. In particular, an acquired somatic mutation at codon 816 in KIT involving an aspartic acid to valine substitution is found in approximately 90% of patients with systemic mastocytosis (SM) and in approximately 40% of patients with core–binding factor acute myeloid leukemia (AML) (1–3). The presence of this mutation in SM and AML is associated with poor prognosis and overall survival. In mice, the expression of this mutation is sufficient to recapitulate several cardinal features of human SM (4). This mutation changes the conformation of the KIT receptor, resulting in altered substrate recognition and constitutive tyrosine autophosphorylation, which leads to a constitutive ligand-independent growth (5–7) that is resistant to imatinib and shows little therapeutic efficacy in response to dasatinib in most SM patients (8, 9). As there are currently no efficacious therapeutic agents against this mutation, we sought to define novel therapeutic targets that might contribute to aberrant signaling downstream from this mutant and which in turn might contribute to the transformation of hematopoietic stem/progenitor cells (HSC/Ps) in diseases such as AML and SM. Previously, we and others have shown that p85α, the regulatory subunit of class IA PI3 kinase (PI3K), is required for KITD814V-induced (murine homolog) transformation (10, 11). Although p85α is a difficult protein to target therapeutically, we hypothesized that perhaps the downstream effectors of the PI3K signaling pathway, in particular guanine exchange factors (GEFs) such as Vav1, Tiam1, and Trio, as well as their downstream targets including the Rho family GTPases Rac1 and Rac2 and p21–activated kinase (Pak), might contribute to gain-of-function mutant KIT–mediated transformation.

Expression of the GEF Vav1 is predominantly restricted to the hematopoietic compartment (12). Vav1 consists of multiple domains including a calponin homology domain, a Dbl homology domain, a pleckstrin homology domain, and a cysteine-rich region, as well as an Src homology 2 (SH2) domain flanked by two SH3 domains (13). Interestingly, deletion of the N-terminal region of Vav1 alone renders this protein oncogenic (12). Although Vav has been shown to play an important role in regulating T and B cell signaling and neutrophil functions (14, 15), its role in leukemogenesis, particularly in oncogenic KIT–induced myeloproliferative neoplasms (MPNs), is unknown. Furthermore, in the context of an oncogene such as *KITD814V*, it is unclear to what extent Vav1 regulates the activation of Rac (Rac1 and Rac2) GTPases and to what extent Rac1 and Rac2 contribute to transformation either alone or via downstream substrates such as Pak.

Rac GTPases cycle between inactive GDP-bound and active GTP-bound states. Rac2 is predominantly expressed in hematopoietic cells, whereas Rac1 is ubiquitously expressed (16). Although the role of Rac1 and Rac2 in normal hematopoiesis has been well documented (16), how these GTPases contribute to oncogenic KIT–induced (KITD814V-induced) transformation is poorly understood. A small-molecule antagonist of Rac, NSC23766 has been described (17). NSC23766 inhibits the activation of Rac by interfering with the binding of GEFs Tiam1 and Trio (17). More recently, Ortiz et al. described a novel Rac inhibitor, EHop-016, which is derived on the basis of the structure of NSC23766 and inhibits the activation of Rac with a substantially

**Authorship note:** Holly Martin, Raghuveer Singh Mali, Peilin Ma, Anindya Chatterjee, and Baskar Ramdas contributed equally to this work.

**Conflict of interest:** The authors have declared that no conflict of interest exists.

**Citation for this article:** *J Clin Invest.* 2013;123(10):4449–4463. doi:10.1172/JCI67509.

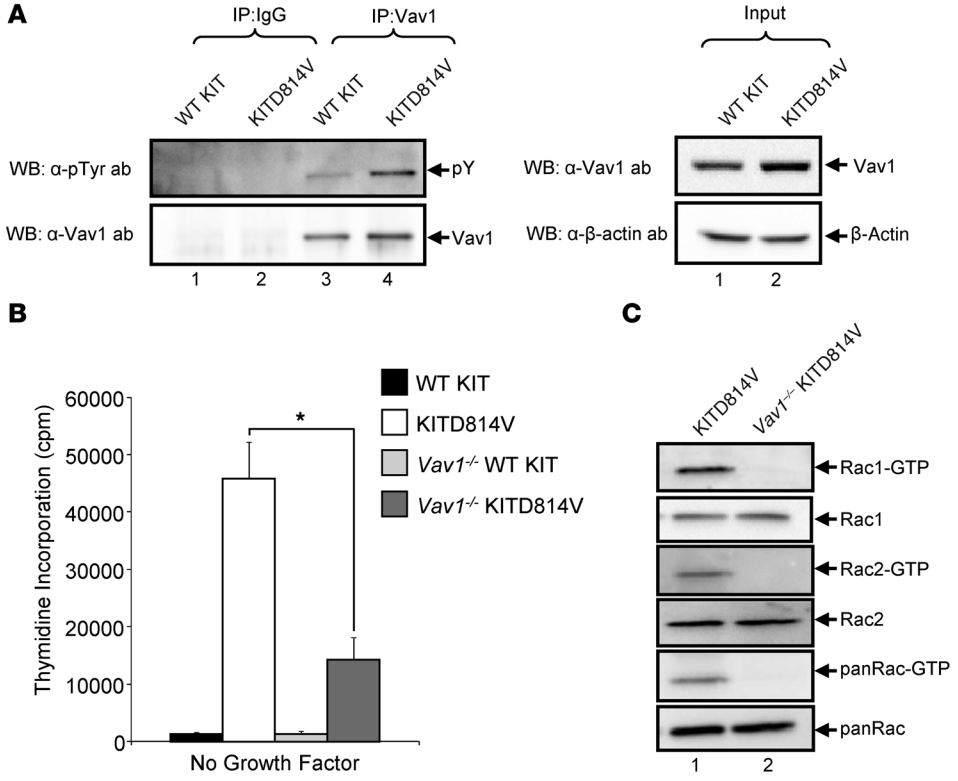


**Figure 1**

Constitutive activation of GEF Vav1 and Rac GTPase in KITD814V-expressing cells. (**A**) 32D cells expressing either WT KIT or KITD814V were serum and growth factor starved for 8 hours, and equal amounts of lysates were subjected to IP using an anti-Vav1 antibody. The position of tyrosine phosphorylated Vav1 is indicated at the right of the blot. Right panel indicates the Vav1 protein whole-cell lysate loading control. (**B**) Proliferation as assessed by thymidine incorporation in KITD814V-expressing WT and Vav1-deficient primary BM cells in the absence of growth factors. Bars represent the mean thymidine incorporation (cpm) in primary BM cells expressing the indicated receptors. Similar results were observed in three independent experiments. *$P < 0.05$ for KITD814V versus *Vav1*$^{-/-}$ KITD814V. (**C**) Cell lysates derived in **B** were analyzed for Rac-GTP levels by incubating with agarose beads conjugated to the Pak binding domain and by subjecting the IPs to Western blot analysis using an anti-Rac1, anti-Rac2, or anti–pan Rac antibody. Rac-GTP position is indicated at the right of the blot. Bottom panel shows total Rac protein in each lane.

lower $IC_{50}$ compared with NSC23766 (18). How these two drugs impact the relative growth of KITD814V-bearing cells and whether they equally inhibit the activation of Rac1 versus Rac2 in these cells has never been explored.

Paks are serine/threonine kinases (19, 20). As a major downstream effector of Rac, Paks play an essential role in regulating both growth and actin-based functions (21–23). Of the three isoforms that belong to the group I family, Pak1 is the most well-characterized member and is ubiquitously expressed (19). Pak1 expression is upregulated in several solid tumors including those in ovarian, breast, and bladder cancers (24–26). While Pak has been shown to function as a potential downstream target of Rac, its relative contribution to MPNs or AML has not been explored. Here, we show that KITD814V-bearing (mouse) and KITD816V-bearing (human) leukemic cells exhibit constitutive activation of Pak, Rac GTPases, and the GEF Vav1. In a series of experiments using knockout mouse models, mouse models of MPN, dominant-negative approaches, an allosteric inhibitor of Pak, and a novel small-molecule inhibitor of Rac, we provide evidence of a mechanism of KITD814V-induced transformation and potentially novel therapeutic targets for the treatment of oncogenic KIT–bearing neoplasms.

## Results

*The GEF Vav1 regulates ligand-independent growth and Rac1 and Rac2 activation in oncogene KIT–bearing (KITD814V-bearing) cells*. The role of hematopoietic-specific GEF and its downstream substrates including Rac1 and/or Rac2 and Pak in KITD814V-induced transformation is not known. To assess whether KITD814V-bearing cells activate the GEF Vav1, we transduced 32D myeloid cells lacking the expression of the endogenous KIT receptor with a bicistronic retrovirus encoding either a WT version of KIT or an oncogenic version (KITD814V) (27). Transduced cells were sorted to homogeneity on the basis of EGFP expression and used in the experiments described here. As seen in Figure 1A, transduced cells bearing KITD814V following 8 hours of serum and growth factor deprivation demonstrated constitutive phosphorylation of Vav1 relative to WT KIT–expressing cells. To assess the functional significance of constitutive Vav1 phosphorylation in KITD814V-bearing primary HSC/Ps, we transduced low-density BM cells derived from WT or *Vav1*$^{-/-}$ mice with EGFP-expressing WT KIT or KITD814V retrovirus. Primary BM cells transduced at similar efficiency were sorted to homogeneity on the basis of EGFP expression and subjected to ligand-independent (in the absence of stem cell factor) growth. As expected and previously shown (27 ), KITD814V-expressing HSC/Ps showed a significant increase in ligand-independent growth compared with WT KIT–bearing cells, however, lack of Vav1 in these cells resulted in approximately 75% repression of ligand-independent growth (Figure 1B). Loss of Vav2 or Vav3 in primary HSC/Ps did not profoundly impact the ligand-independent growth of KITD814V-bearing cells (Supplemental Figure 1; supplemental material available online with this article; doi:10.1172/JCI67509DS1).

To assess how Vav1 might contribute to KITD814V-induced ligand-independent growth, we determined the activation status of downstream substrates of Vav1, the Rac family GTPases (16, 28). We examined the activation of both Rac1 and Rac2 in Vav1-deficient KITD814V-bearing HSC/Ps. Figure 1C shows the constitutive activation of both Rac1 and Rac2 in KITD814V-bearing WT HSC/Ps. In contrast, the activation of both Rac1 and Rac2 was reduced in KITD814V-bearing *Vav1*$^{-/-}$ HSC/Ps. These results suggest that Vav1 regulates Rac1 and Rac2 activation to a similar extent in

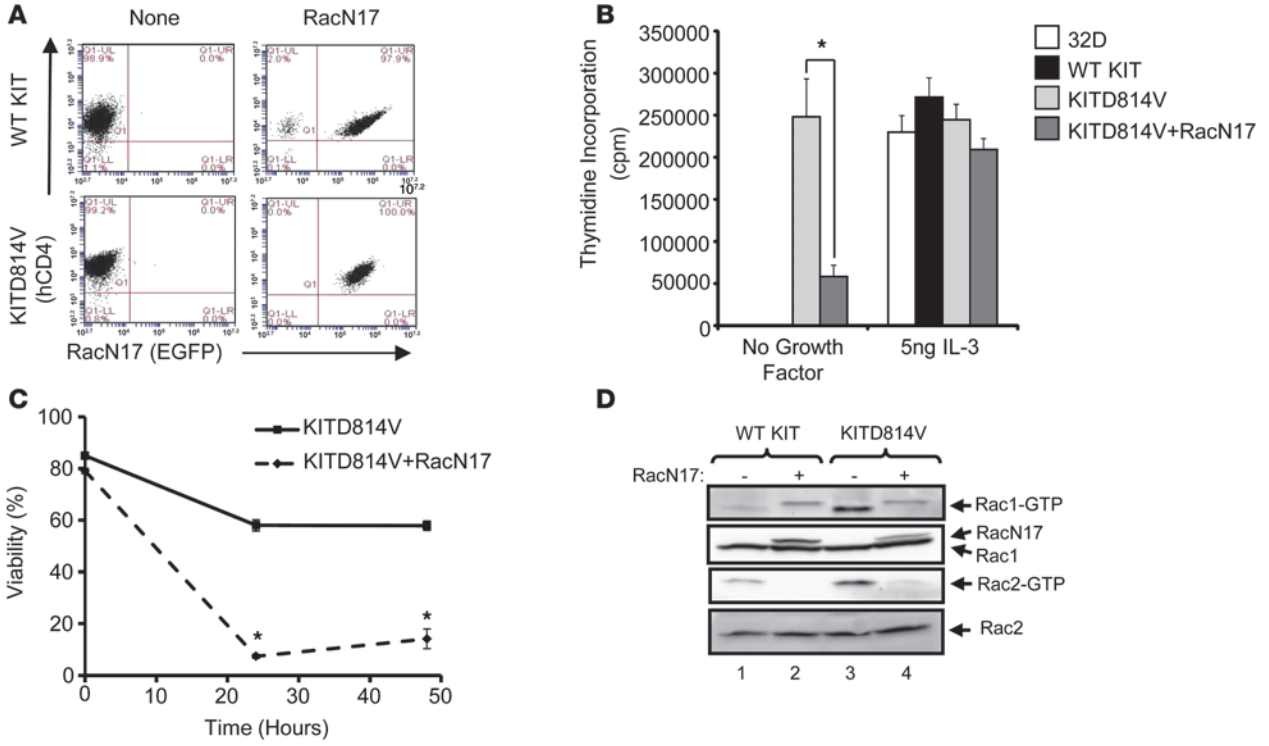


**Figure 2**

Inhibition of Rac activity in KITD814V-bearing cells suppresses cell growth and survival. (**A**) Flow cytometric analysis of 32D myeloid cells expressing WT KIT-hCD4 or KITD814V-hCD4 (*y* axis) and dominant-negative RacN17-EGFP (*x* axis). (**B**) Cells expressing KITD814V with or without RacN17 were cultured for 48 hours in the presence or absence of IL-3 in replicates of four and were subjected to a [$^3$H] thymidine incorporation assay. Bars represent the mean ± SD thymidine incorporation (cpm). Similar results were observed in three independent experiments. **P* < 0.05 for KITD814V versus KITD814V plus RacN17. (**C**) Cells in **B** were grown in the absence of growth factors for 24 or 48 hours prior to being subjected to annexin V and 7-AAD staining. Survival (viability) was determined as the percentage of both annexin V– and 7-AAD–negative cells. Bars denote the mean ± SD percentage of total surviving cells from one of two independent experiments performed in quadruplicate. **P* < 0.05 for KITD814V versus KITD814V plus RacN17. (**D**) Cells in **B** were subjected to a Pak–binding domain (PBD) pulldown assay to assess Rac1 GTP, Rac2 GTP, total Rac1, and total Rac2 expression in the indicated genotypes. Data are from a representative experiment performed on three separate occasions.

KITD814V-bearing cells and that deficiency of Vav1 in KITD814V-bearing cells significantly reduces the ligand-independent growth normally associated with these cells.

While these results suggest a role for Vav1 in Rac activation and perhaps in KITD814V-induced transformation, its direct involvement can only be established by inhibiting the activation of Rac in these cells. To test this, we infected KITD814V-bearing 32D myeloid cells with a dominant-negative version of Rac (RacN17). A bicistronic retrovirus encoding WT KIT or KITD814V along with a human CD4 antigen as a selectable marker was used for these studies (Figure 2A). RacN17 was cloned into an EGFP-enconding retrovirus (for selection of transduced cells). 32D myeloid cells were coinfected with virus encoding WT KIT or KITD814V and/or RacN17. Cells were sorted on the basis of hCD4 and/or EGFP expression (Figure 2A). Single- or double-positive sorted cells were subjected to a proliferation assay. As seen in Figure 2B, the expression of a dominant-negative version of Rac (RacN17) in KITD814V-bearing cells significantly repressed ligand-independent growth relative to controls. The reduction in the growth of KITD814V- and RacN17-coexpressing cells was in part due to reduced survival relative to controls (Figure 2C). IL-3 responses in all of these cell types, including in KITD814V- and RacN17-coexpressing cells, were comparable (Figure 2B). The reduction in the growth and survival of KITD814V- and RacN17-coexpressing cells was due to the direct repression of Rac1 and Rac2 (Figure 2D). Taken together, these results suggest that downstream from Vav1, Rac1 and Rac2 likely play an essential role in regulating KITD814V-induced transformation.

To test this in more detail, we performed transplant studies by injecting myeloid cells coexpressing KITD814V and RacN17 along with control cells into C3H/HeJ syngeneic mice (27). Transplanted mice were observed for the development of MPNs and survival relative to controls. Mice transplanted with cells coexpressing KITD814V and RacN17 demonstrated a significantly prolonged lifespan relative to the KITD814V-only–expressing mice (Figure 3A). To assess the impact of Rac repression on MPN development, a cohort of KITD814V- and RacN17-coexpressing mice were analyzed in detail at the same time as when the KITD814V-only–bearing mice first began to succumb. As seen in Figure 3B, KITD814V-bearing mice showed peripheral blood (PB) counts in the range of 150 K/μl. In contrast, mice transplanted with cells coexpressing KITD814V and RacN17 demonstrated a profound reduction in PB wbc and neutrophil (NE) counts. Additional analysis was conducted on KITD814V- and RacN17-coexpressing mice when

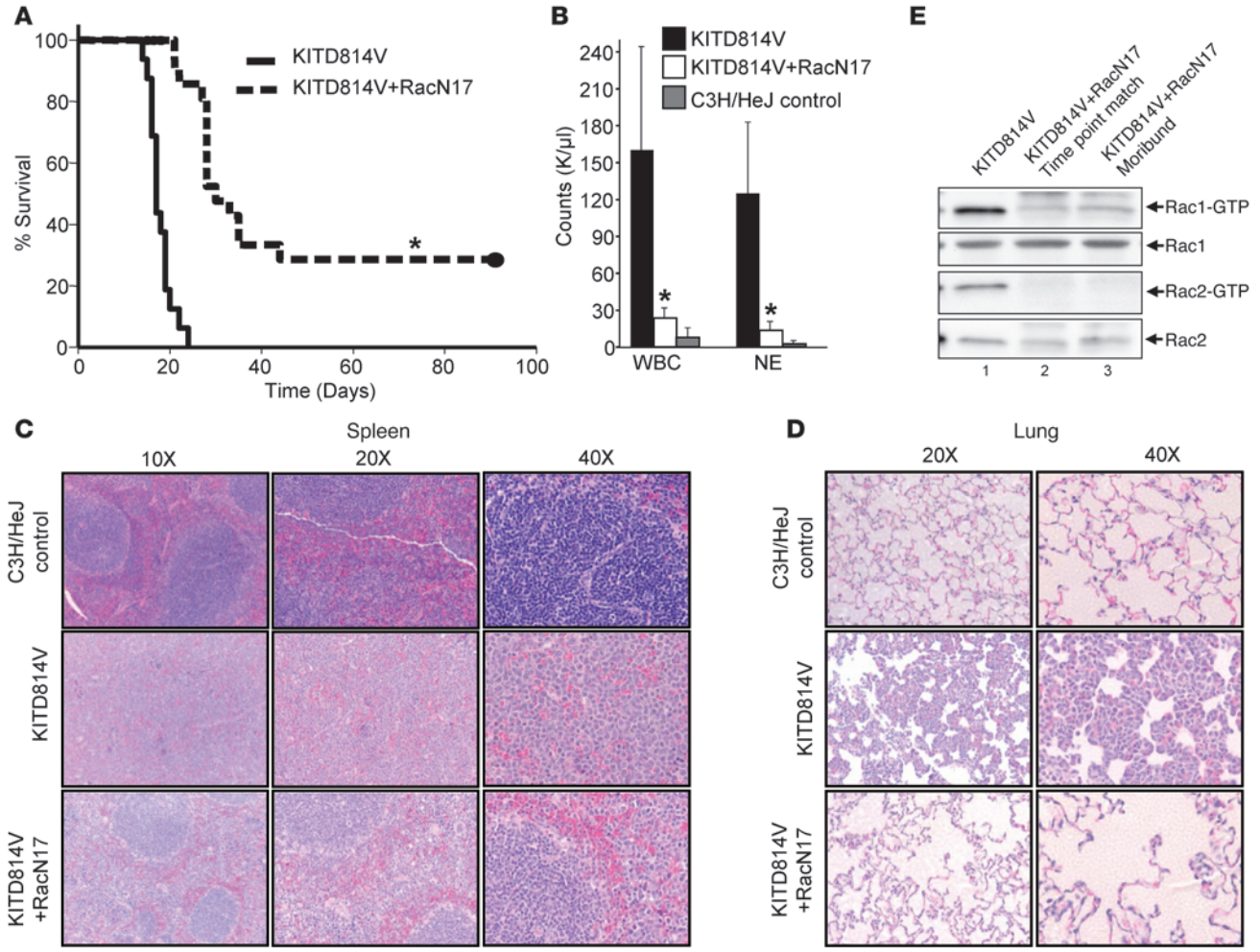


**Figure 3**

In vivo inhibition of Rac prolongs survival and rescues myeloid cell infiltration associated with KITD814V-bearing mice. C3H/HeJ mice were transplanted with 2 million cells bearing KITD814V, with or without RacN17. (**A**) Kaplan-Meier survival analysis of syngeneic C3H/HeJ mice transplanted with cells bearing KITD814V ($n = 16$) or KITD814V plus RacN17 ($n = 26$). *$P < 0.001$ for KITD814V versus KITD814V plus RacN17. (**B**) White blood cell (WBC) and NE counts in mice bearing cells transplanted with KITD814V ($n = 9$) or KITD814V plus RacN17 ($n = 12$) and C3H/HeJ control mice ($n = 5$). *$P < 0.05$ for KITD814V versus KITD814V plus RacN17. Histopathologic analysis of spleen (**C**) and lung (**D**) from mice transplanted with cells bearing KITD814V alone or in combination with RacN17. Shown are representative tissue sections after fixing them in 10% buffered formalin, sectioning them, and staining them with H&E. Original magnification, ×10 (left panels), ×20 (center panels), and ×40 (right panels). Normal erythroid and myeloid components in lungs, liver, and spleen were replaced by leukemic cells in KITD814V-bearing mice, which were significantly rescued in tissues from mice bearing RacN17 along with KITD814V. (**E**) Cell lysates derived from spleens of mice described above were subjected to a Rac activity assay as described in Figure 2. Shown is the level of Rac1 GTP, Rac2 GTP, total Rac1, and total Rac2 in each lane from the indicated genotypes.

the KITD814V-only mice began to succumb. In other words, KITD814V- and RacN17-bearing mice were sacrificed at the same time as the moribund KITD814V mice to assess disease progression and the impact of Rac repression on MPNs. Around the time of death, up to 90% of the leukemic cells were detected in the PB, BM, and spleen of mice transplanted with cells bearing KITD814V alone (Supplemental Figure 2A). In contrast, mice transplanted with cells coexpressing KITD814V and RacN17 demonstrated only approximately 20% leukemic cells as determined by EGFP positivity in all three tissues examined. The left panel of Supplemental Figure 2A shows a quantitative assessment of the presence of EGFP-expressing cells in PB, BM, and spleen, and the right panel shows representative flow cytometric blots demonstrating the percentage of EGFP expression in various tissues in the indicated genotypes. Supplemental Figure 2B demonstrates a quantitative reduction in the spleen weight of mice transplanted with cells coexpressing KITD814V and RacN17 relative to mice transplanted with cells bearing the KITD814V mutation alone. The right panel depicts representative spleens derived from KITD814V-bearing mice as well as mice coexpressing KITD814V and RacN17. Importantly, while gross lung lesions were observed in mice transplanted with cells bearing KITD814V alone, these lesions were nearly absent in the lungs of transplanted mice coexpressing KITD814V and RacN17 (Supplemental Figure 2C). Histopathological analysis revealed that while massive myeloid cell infiltration was observed in mice transplanted with KITD814V-bearing cells in spleen and

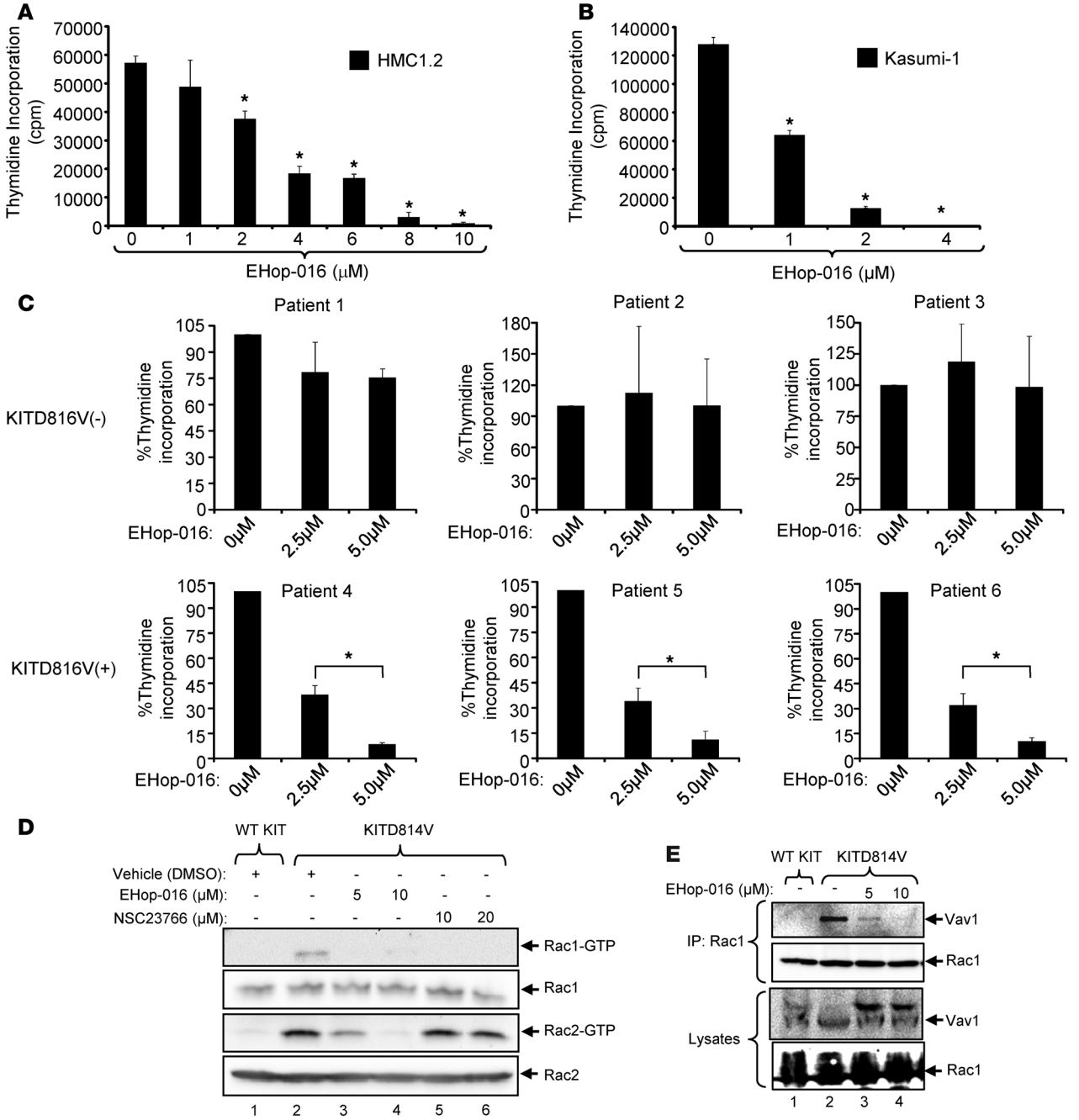


**Figure 4**

A novel Rac inhibitor, EHop-016, is a potent inhibitor of KITD814V-induced growth in SM and AML patient–derived cells. (**A**) Human SM patient–derived HMC1.2 cells bearing KITD816V and (**B**) human AML patient–derived Kasumi-1 cells bearing KITD816V were cultured in the presence of EHop-016 and assessed for proliferation by measuring [$^3$H] thymidine incorporation. Bars represent the mean ± SD from four independent experiments performed in replicates of four; *$P < 0.05$. (**C**) Individual SM patient–derived cells positive or negative for KITD816V expression were cultured in the presence of the indicated concentrations of EHop-016. Bars represent the mean ± SD performed in replicates of three. *$P < 0.05$; 0 μM versus the indicated concentration. (**D**) 32D cells bearing WT KIT or KITD814V were starved and treated with the indicated concentrations of NSC23766 or EHop-016 and subjected to Rac activation assay. Shown are the levels of active Rac1, Rac2, total Rac1, and Rac2 in each lane. (**E**) 32D cells expressing either WT KIT or KITD814V were starved and incubated with vehicle, 5 μM or 10 μM EHop-016; lysates were immunoprecipitated with anti-Rac1 antibody and immunoblotted with an anti-Vav1 or anti-Rac1 antibody, respectively. Lower panels indicate the Vav1 and Rac1 protein whole-cell lysate loading control.

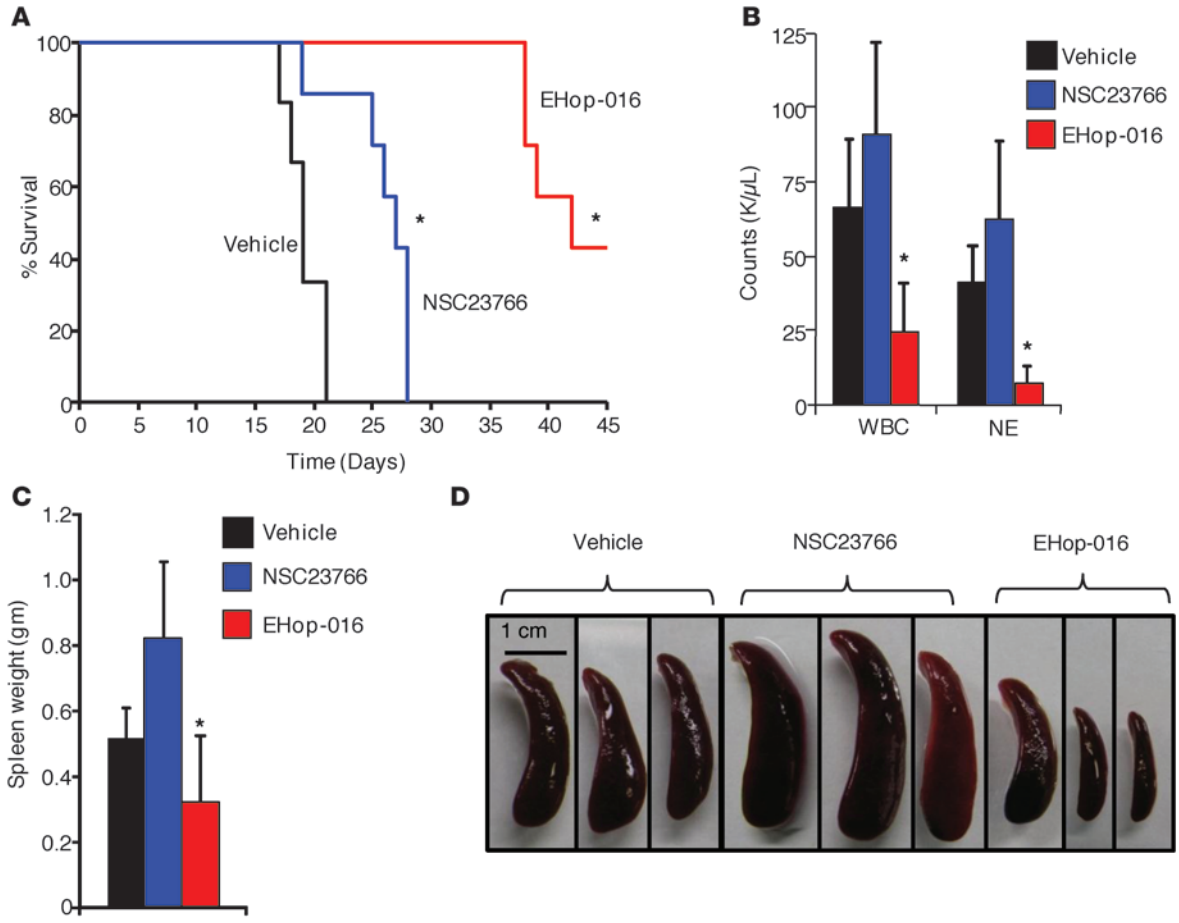


**Figure 5**

Pharmacologic inhibition of Rac GTPases delays disease progression in mice transplanted with cells bearing the KITD814V receptor. C3H/HeJ mice were transplanted with 1 million cells bearing KITD814V following overnight treatment with vehicle ($n = 6$), EHop-016 (2.5 μM, $n = 7$), or NSC23766 (25 μM, $n = 7$), and (**A**) survival was analyzed by Kaplan-Meier log-rank analysis. *$P < 0.05$ for vehicle versus EHop-016 or NSC23766. (**B**) PB counts for wbcs and NEs between the different transplanted groups at the time of harvest. *$P < 0.05$ for vehicle versus EHop-016. (**C**) Quantitative difference in spleen mass and (**D**) representative spleens from indicated transplantation groups are shown. *$P < 0.05$ for vehicle versus EHop-016.

lungs, mice bearing cells coexpressing KITD814V and RacN17 showed markedly less infiltration of these cells, and the splenic architecture in these mice was indistinguishable from the control mice (Figure 3, C and D).

To assess whether the enhanced survival of mice, the reduced infiltration of myeloid blasts in various tissues including lung and liver, and the lack of destruction of the splenic architecture observed in mice transplanted with cells coexpressing KITD814V and RacN17 were due to reduced Rac activation, we examined the activation status of Rac1 and Rac2 in splenocytes. Cellular lysates from spleens of KITD814V-bearing mice were harvested at moribundity. At the same time, splenic lysates were derived from mice transplanted with cells coexpressing KITD814V and RacN17, designated as time point matched and moribund, respectively. As seen in Figure 3E, mice transplanted with cells coexpressing RacN17 and KITD814V showed marked repression in both Rac1 and Rac2 activation compared with controls. In addition to Rac repression, a substantial repression in the activation of Pak, a downstream substrate of Rac, was also observed (Supplemental Figure 3). These results suggest that expression of RacN17 in KITD814V-bearing cells likely inhibits their growth in vivo by inhibiting the activation of Rac1 and Rac2, resulting in prolonged survival and delayed MPN development.

*Growth of oncogenic KIT-bearing (KITD814V in mouse and KITD816V in humans) murine and human mastocytosis patient–derived cells is inhibited by a novel Rac inhibitor, EHop-016.* Based on the observation that Rac inhibition in vivo delays KITD814V-driven MPN, we hypothesized that pharmacologic inhibition of Rac might inhibit KITD814V-induced proliferation in vitro. For these studies, we first used the well-characterized Rac inhibitor NSC23766 (17). NSC23766 inhibits Rac binding and activation by the Rac-specific GEFs Trio and Tiam1 (17). Treatment of myeloid cells bearing the WT KIT or KITD814V receptor with NSC23766 demonstrated a dose-dependent reduction in the hyperproliferation of KITD814V-bearing cells but not of WT KIT–bearing cells (Supplemental Figure 4A). Treatment of the murine mastocytoma cell line P815, which bears the activating KITD814V mutation, as well as treatment of AML patient–derived Kasumi-1 cells, which express the KITD816V mutation, consistently demonstrated dose-dependent growth repression in the presence of NSC23766 (Supplemental Figure 4, B and C). While dose-dependent growth inhibition of

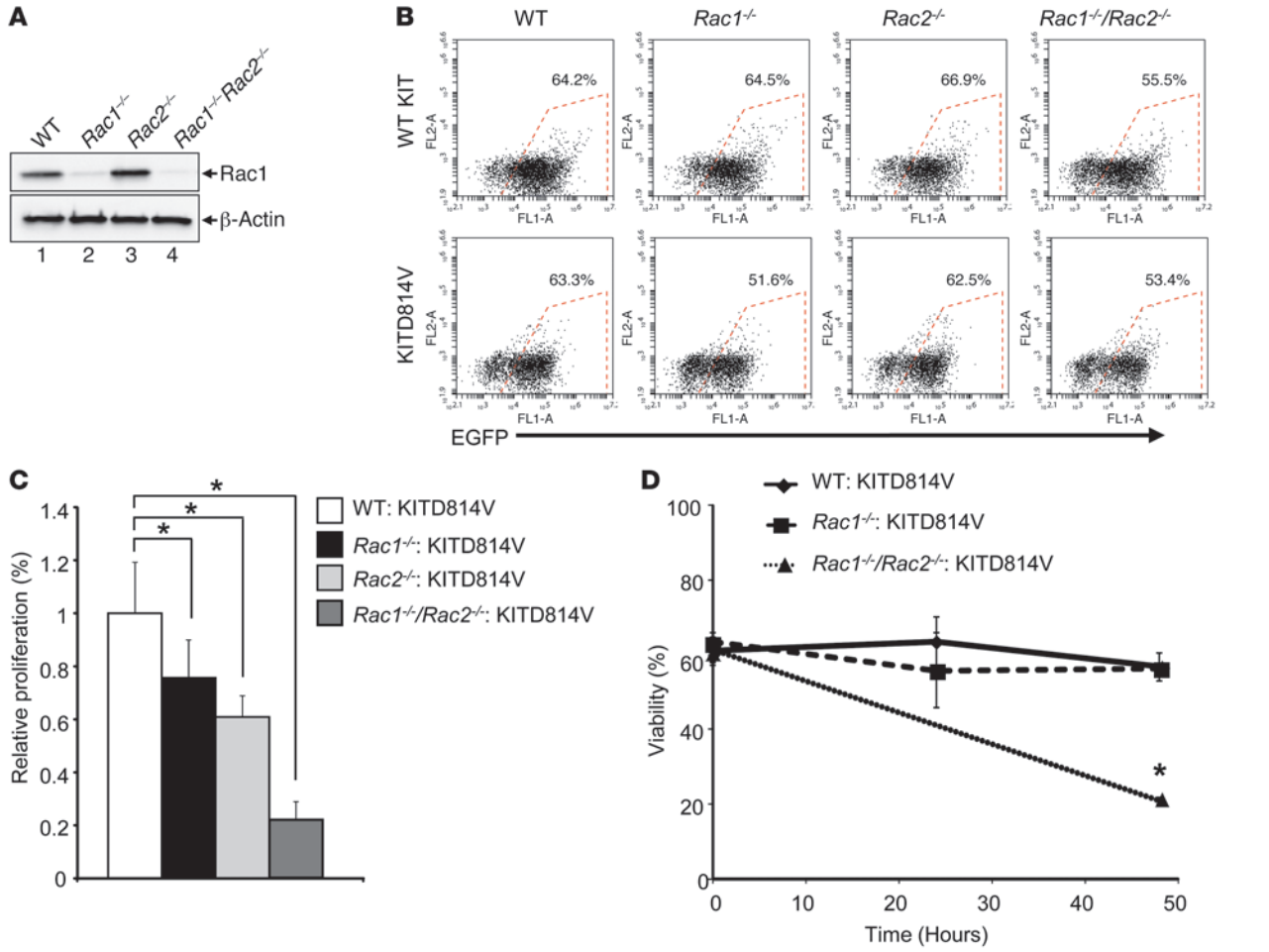


**Figure 6**

Deficiency of Rac1 and Rac2 in KITD814V-bearing primary HSC/Ps represses ligand-independent growth. (**A**) PB cells were collected from WT, *Rac1*$^{flox/flox}$, *Rac2*$^{-/-}$, and *Rac2*$^{-/-}$/*Cre:Rac1*$^{flox/flox}$ mice following four consecutive i.p. injections of polyI:C given at 48-hour intervals. Red blood cells were lysed, and equal amounts of protein were subjected to Western blotting using an anti-Rac1 antibody. Levels of Rac1 in each lane are shown. (**B**) Representative flow cytometric dot plots of low-density BM cells derived from WT, *Rac1*$^{-/-}$, *Rac2*$^{-/-}$, and *Rac1*$^{-/-}$/*Rac2*$^{-/-}$ mice transduced with WT KIT– or KITD814V-expressing retrovirus. EGFP expression on the *x* axis is reflective of the transduction efficiency in the indicated genotypes. (**C**) WT, *Rac1*$^{-/-}$, *Rac2*$^{-/-}$, and *Rac1*$^{-/-}$/*Rac2*$^{-/-}$ primary HSC/Ps expressing WT KIT or KITD814V were subjected to a thymidine incorporation assay. **P* < 0.05 for KITD814V in WT versus *Rac2*$^{-/-}$, *Rac1*$^{-/-}$, or *Rac1*$^{-/-}$/*Rac2*$^{-/-}$ cells. Shown are the combined data from three independent experiments in replicates of four. (**D**) WT, *Rac1*$^{-/-}$, and *Rac1*$^{-/-}$/*Rac2*$^{-/-}$ primary HSC/Ps expressing KITD814V were grown in the absence of growth factors for 0, 24, or 48 hours prior to being analyzed by annexin V and 7-AAD staining. Apoptosis was determined as a percentage of both annexin V– and 7-AAD–positive staining. Bars denote the mean ± SD percentage of annexin V– and 7-AAD–negative (viable) cells. **P* < 0.05 for WT, *Rac1*$^{-/-}$ versus *Rac1*$^{-/-}$/*Rac2*$^{-/-}$.

oncogene KIT–bearing cells in the presence of NSC23766 was observed, the concentration of NSC23766 that resulted in 50% growth inhibition of leukemic cells was nearly 75 to 100 μM for all cell types examined. This could potentially be due to a lack of a major role of the GEFs Trio and Tiam1 in KITD814V-induced transformation. Alternatively, Rac1 and/or Rac2 alone may play only a modest role in KITD814V-induced transformation. To test these possibilities and to more precisely identify the consequence(s) of interfering with the function of GEFs and Rac in KITD814V-induced transformation, we used a novel Rac inhibitor, EHop-016, which is a derivative of NSC23766 and inhibits Rac 100-fold more efficiently than NSC23766 in breast cancer cell lines (18). As seen in Figure 4, A and B, KITD816V-bearing SM patient–derived HMC1.2 cells, as well as KITD816V- and AML1-ETO–bearing Kasumi-1 cells derived from an AML patient, demonstrated a significant reduction in the growth of these cells in the presence of EHop-016 at drug concentrations that were significantly less (~50-fold in some cases) than those of NSC23766. Importantly, primary SM patient–derived cells bearing KITD816V were significantly more susceptible to growth inhibition in the presence of EHop-016 relative to patient samples lacking the expression of KITD816V (Figure 4C). The growth reduction in the presence of EHop-016 was also observed in murine KITD814V–expressing cells and was associated with enhanced apoptosis and repression of antiapoptotic proteins BAD and MLC (Supplemental Figure 4, D–F). Consistent with these findings, while 20 μM of NSC23766 inhibited the activation of Rac1 but not Rac2 in KITD814V-bearing cells, 10 μM of EHop-016 was sufficient to

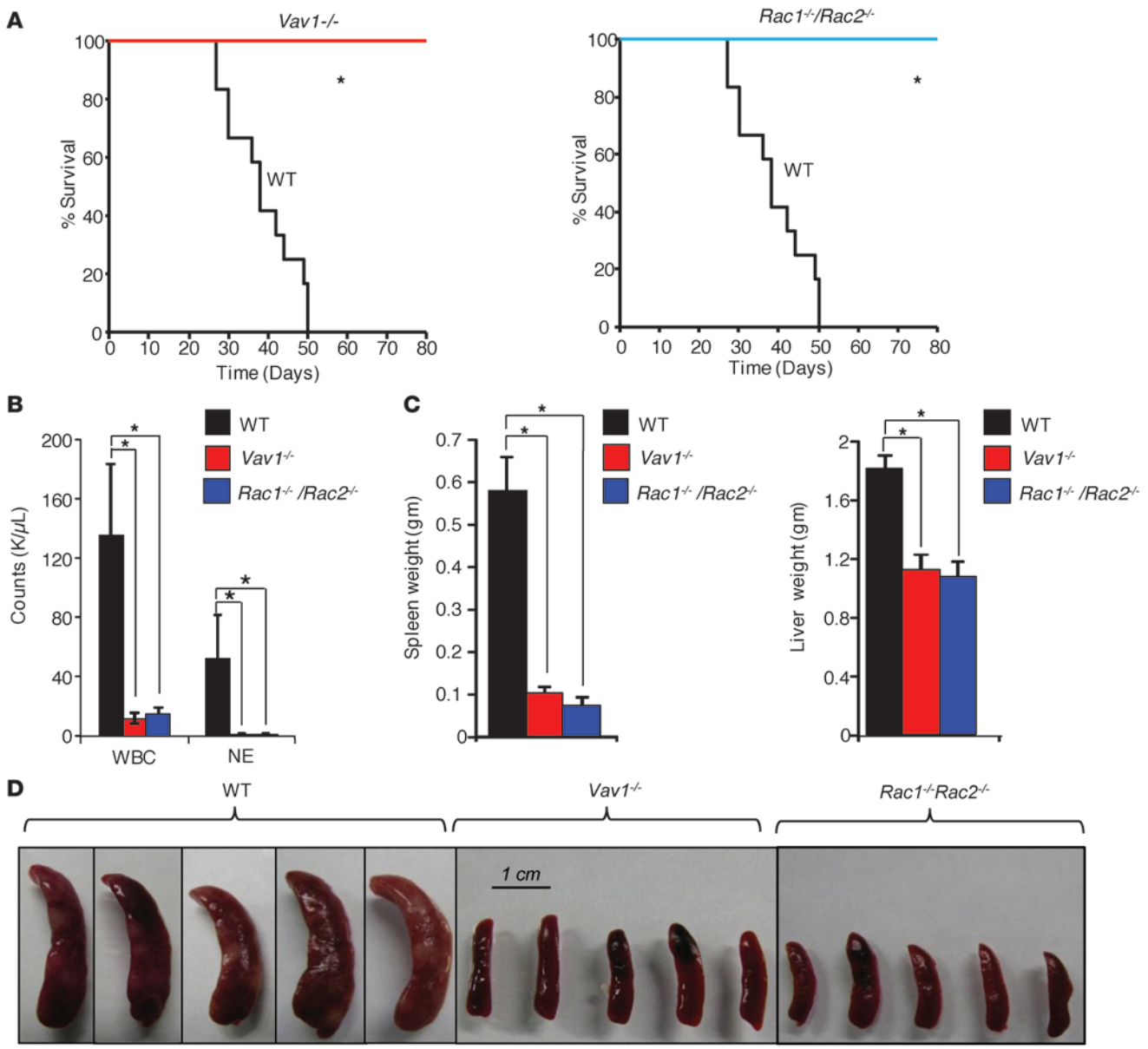


**Figure 7**

Genetic disruption of GEF Vav1 and Rac GTPases enhances the survival of KITD814V-bearing mice. (**A**) Cumulative survival analysis using a Kaplan-Meier log-rank test in recipient mice bearing KITD814V-expressing WT ($n$ = 10), *Vav1*$^{-/-}$ ($n$ = 5), or *Rac1*$^{-/-}$/*Rac2*$^{-/-}$ ($n$ = 5) HSC/Ps. *$P$ < 0.05 for WT versus *Vav1*$^{-/-}$ or *Rac1*$^{-/-}$/*Rac2*$^{-/-}$. (**B**) PB counts were significantly elevated in recipients of KITD814V-bearing WT HSC/Ps ($n$ = 10) relative to KITD814V-bearing *Vav1*$^{-/-}$ ($n$ = 5) or *Rac1*$^{-/-}$/*Rac2*$^{-/-}$ ($n$ = 5) HSC/Ps. *$P$ < 0.05 for WT versus *Vav1*$^{-/-}$ or *Rac1*$^{-/-}$/*Rac2*$^{-/-}$: KITD814V. Data are the mean ± SEM. (**C**) Quantitative difference in the size of the spleen and liver between different transplanted groups. *$P$ < 0.05 for WT versus *Vav1*$^{-/-}$ or *Rac1*$^{-/-}$/*Rac2*$^{-/-}$. (**D**) Representative spleen pictures derived from mice transplanted with HSC/Ps bearing KITD814V in the setting of the indicated genotypes.

inhibit the activation of both Rac1 and Rac2 in these same cells, which was associated with reduced binding of Vav to Rac (Figure 4, D and E). These results suggest that inhibition of both Rac1 and Rac2 is essential for maximal growth repression in KITD814V-bearing cells. Further, the Rac inhibitor EHop-016 is substantially more efficient at repressing the growth and activation of Rac1 and Rac2 in KITD814V-bearing cells compared with NSC23766. Consistent with the in vitro findings described above, the treatment of KITD814V-bearing cells with EHop-016 versus NSC23766 significantly enhanced the survival of leukemic mice, as demonstrated by reduced spleen size and PB counts (Figure 5, A–D).

*Genetic disruption of Rac GTPases in KITD814V-bearing HSC/Ps inhibits ligand-independent hyperproliferation and MPNs in vivo.* We next analyzed the specific role of Rac1 and Rac2 and also attempted to confirm our findings using dominant-negative Rac (RacN17) and pharmacologic approaches by examining the growth of KITD814V-bearing primary BM cells derived from mice lacking the expression of Rac1, Rac2, or both Rac1 and Rac2. Since complete loss of

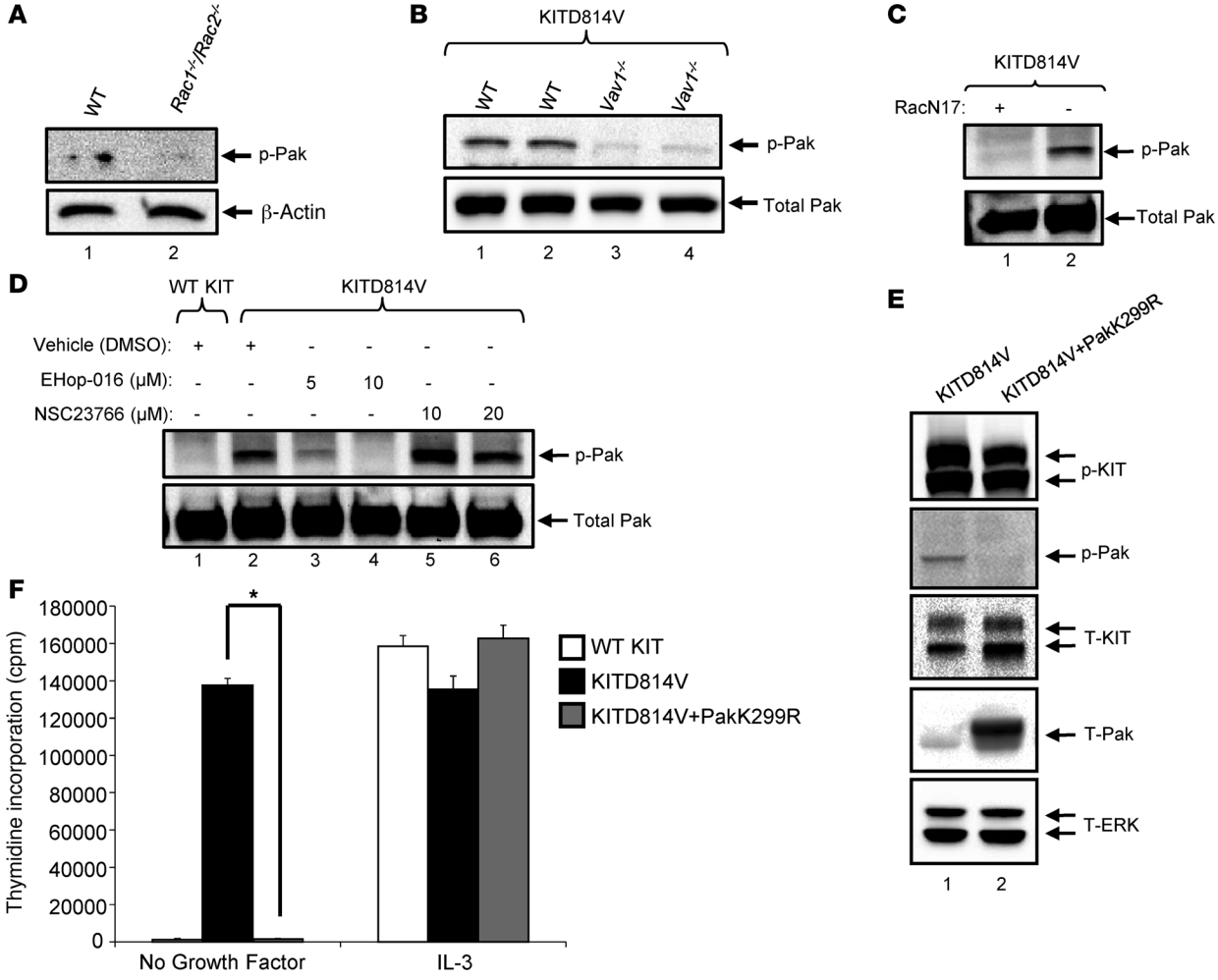


**Figure 8**

KITD814V induces the activation of Pak in a Vav1- and Rac-dependent manner. KITD814V-expressing WT or Rac1/Rac2 (**A**) or Vav1-deficient primary HSC/Ps (**B**) from two independent animals were starved and lysed and immunoblotted for active Pak. (**C**) KITD814V-bearing 32D cells expressing RacN17 were starved and lysed, and equal amounts of lysates were subjected to immunoblotting using a phospho-Pak antibody and total Pak. (**D**) Cells bearing WT KIT or KITD814V were starved and treated with the indicated concentrations of NSC23766 or EHop-016 and subjected to Rac activation assay. Shown are the levels of phosphorylated and total Pak. (**E**) 32D cells were transduced with KITD814V with or without dominant-negative PakK299R and starved; lysates were subjected to Western blot analysis using phospho-KIT, phospho-Pak, total KIT, total Pak, and total ERK antibodies. (**F**) Cells in **E** were starved for 6 hours before being plated in quadruplicate in the presence or absence of growth factors (IL-3, 5 ng/ml) for 48 hours. Cells were pulsed with [$^3$H] thymidine for 6 hours and harvested. Bars denote the mean thymidine incorporation (cpm ± SD) from one of four independent experiments performed in quadruplicate. *$P < 0.05$ for KITD814V versus KITD814V plus PakK299R.

Rac1 results in embryonic lethality, we used a conditional knockout strain of *Rac1*, which was crossed with *Mx1-Cre* mice, allowing for the conditional deletion of Rac1 in BM cells upon treatment with polyI:C (29). As seen in Figure 6A, and has been previously described, the conditional deletion of *Rac1* results in the loss of Rac1 protein. A similar loss of Rac1 protein was also observed in mice lacking both Rac1 and Rac2, as assessed by Western blot analysis using a Rac1-specific antibody (Figure 6A; lanes 2 and 4). Low-density BM cells from all three genotypes were prestimulated with cytokines and infected with a retrovirus expressing WT KIT or KITD814V. Figure 6B shows the transduction efficiency of the two viruses in BM cells derived from different genotypes. Transduced cells were sorted to homogeneity for use in a proliferation assay and to assess survival in the absence of Rac proteins. As seen in Figure 6C, while loss of Rac2 resulted in an approximately 50% inhibition of ligand-independent growth of KITD814V-bearing cells, loss of Rac1 showed only a modest reduction (~10% to 15%). In contrast, BM cells deficient in both Rac1 and Rac2 showed a more profound reduction in the growth of KITD814V-bearing cells (~75%). The reduction in the growth of Rac1/Rac2 double–knockout cells bearing KITD814V was due in part to the reduced survival of cells relative to controls (Figure 6D). These findings suggest that the combined loss of Rac1 and Rac2 results in most of the growth repression seen in KITD814V-bearing cells. Restoring the expression of activated Rac in the setting of Rac1/Rac2 deficiency rescued ligand-independent growth in vitro (Supplemental Figure 5A). Furthermore, no compensatory increase in the expression of Rac3 was noted in these cells (Supplemental Figure 5B). To further assess the role of Vav1 and Rac1/Rac2 in KITD814V-induced MPNs, we infected WT or *Vav1*$^{-/-}$ or *Rac1/Rac2*$^{-/-}$

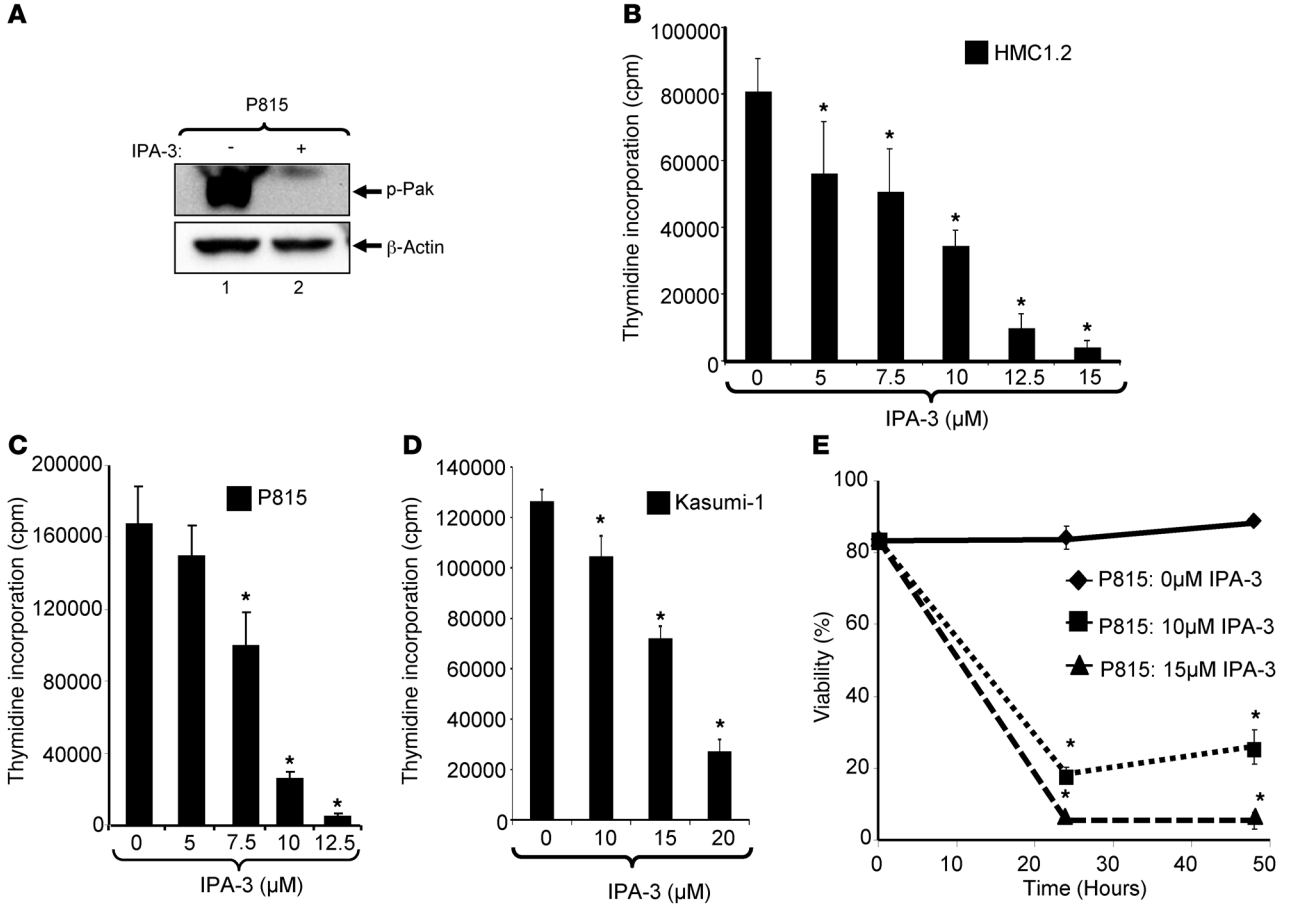


**Figure 9**

Inhibition of constitutively active Pak by IPA-3. (**A**) KITD814V-bearing murine P815 mastocytoma cells were incubated in the presence or absence of 10 μM IPA-3 and subjected to immunoblotting with a phospho-Pak antibody. Levels of phospho-Pak and total protein in each lane are shown. HMC1.2 (**B**), P815 (**C**), and Kasumi-1 (**D**) cells bearing an activating KIT mutation exhibited dose-dependent inhibition when grown in the presence of IPA-3 and were assessed for proliferation by measuring [$^3$H] thymidine incorporation. Bars represent the mean ± SD from two to three independent experiments performed in replicates of three; *$P < 0.05$. (**E**) P815 cells were subjected to an apoptosis assay after treating them with 10 or 15 μM IPA-3 under no growth factor conditions for 24 or 48 hours prior to analyzing them with annexin V and 7-AAD staining. Apoptosis was assessed as a percentage of annexin V– and 7-AAD–positive cells. Bars denote the mean ± SD percentage of total viable cells from one of two independent experiments performed in quadruplicate. *$P < 0.05$; 0 μM versus 10 or 15 μM.

5-FU–treated BM cells with a virus expressing KITD814V, sorted the cells on the basis of EGFP expression, and transplanted them into lethally irradiated hosts. Supplemental Figure 6 shows the transduction efficiency of 5-FU–treated cells in all three genotypes. As seen in Figure 7A, a significant increase in the survival of mice bearing *Vav1*$^{-/-}$ or *Rac1/Rac2*$^{-/-}$ KITD814V–expressing cells was observed relative to controls. Further, we observed the rescue of PB counts and splenomegaly in these mice relative to controls (Figure 7, B–D). The loss of Rac2 alone in the setting of KITD814V expression also prolonged the survival of leukemic mice, but to a much lesser degree compared with mice transplanted with KITD814V-bearing cells lacking the expression of Vav1 or Rac1/Rac2 (Supplemental Figure 7).

*Role of p21-activated kinase in KITD814V-induced transformation*. As noted earlier, the expression of dominant-negative Rac (RacN17) in KITD814V-bearing cells derived from the spleens of transplanted mice not only resulted in reduced Rac1/Rac2 activation, but also inhibited the activation of Pak. The involvement of Pak in MPNs or in leukemogenesis has never been reported, although recent studies have implicated Pak in regulating the growth and actin-based functions in solid tumors (30–32). To assess the role of Pak in KITD814V-induced transformation and to determine whether Pak functions downstream from Vav1 and Rac1/Rac2 in KITD814V-bearing cells, we examined Pak activation in KITD814V-bearing *Vav1*$^{-/-}$, *Rac1/Rac2*$^{-/-}$, RacN17, or EHop-016–treated primary HSC/Ps. As seen in Figure 8, A–D, a reduction in the activation of Pak was observed in every scenario. To assess the direct role of Pak in regulating ligand-independent growth of KITD814V-bearing cells, we used myeloid cells bearing the expression of KITD814V and infected them with a retrovirus expressing a dominant-negative version of Pak (PakK299R). One-hundred percent of the EGFP (reflecting the expression of PakK299R) and hCD4 (reflecting the expression of KITD814V) double-positive cells were sorted to homogeneity and subjected to a biochemical and proliferation assay as described in Figure 2 (Supplemental Figure 8A). As seen in Figure 8E, while the expression of KIT and

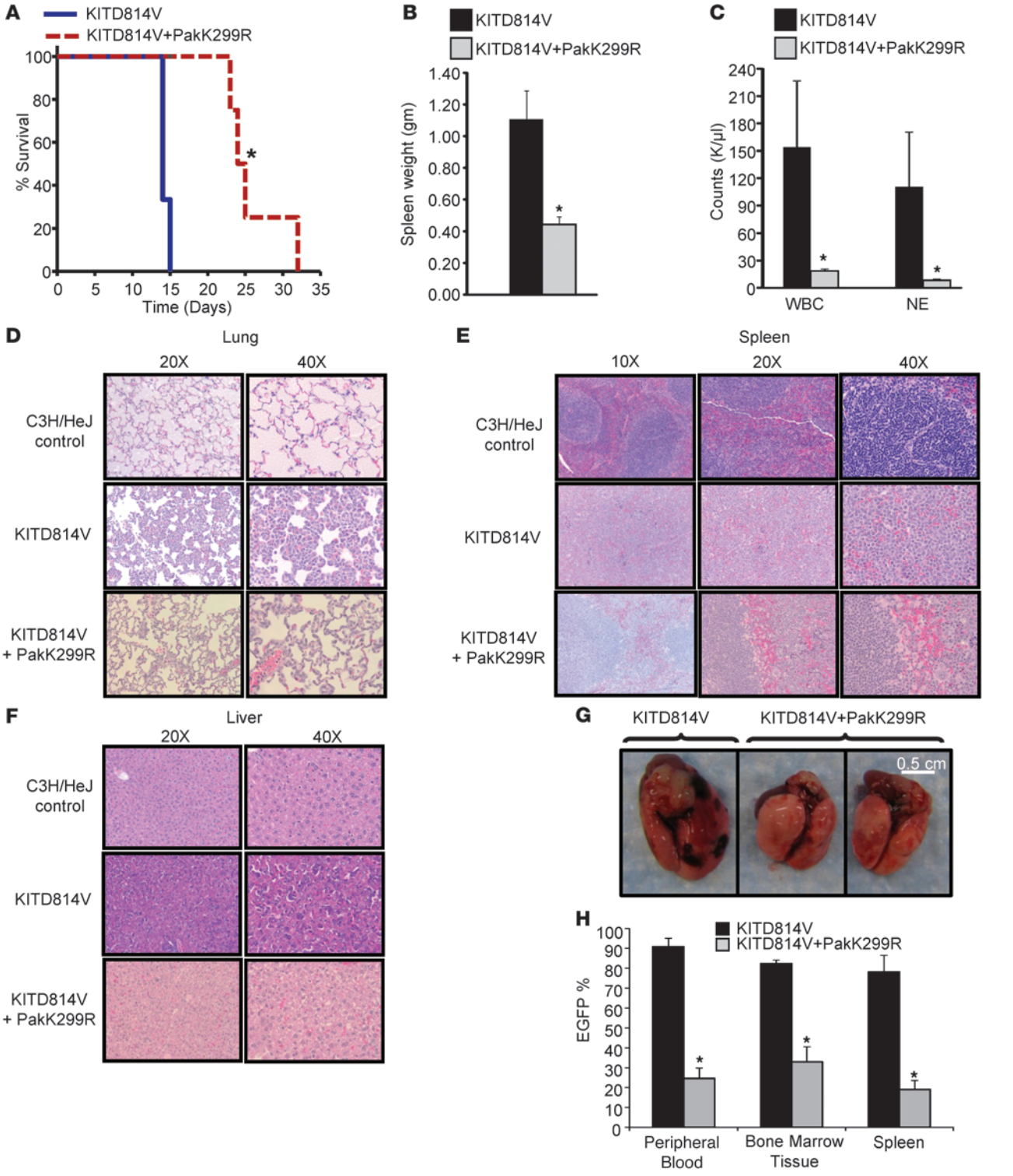


**Figure 10**

Inhibition of Pak in vivo in KITD814V-bearing mice enhances survival and significantly delays the development of MPNs. (**A**) Kaplan-Meier survival curves of mouse cohorts transplanted with either 32D cells bearing KITD814V alone or in combination with Pak299R. Survival of recipients with Pak299R was significantly prolonged compared with KITD814V-only transplanted mice ($n = 3$ to 4; $^*P < 0.01$). Repression of Pak in vivo in KITD814V-bearing cells results in a significant decrease in spleen weight (**B**) and PB counts (**C**) relative to controls ($n = 3$, $^*P < 0.05$). (**D**–**F**) Lungs, spleens, and livers from the indicated genotypes were subjected to histopathological analysis. Shown are representative tissue sections. Original magnification, ×20 to ×40, as shown. (**G**) Representative pictures of intact lungs from mice bearing KITD814V alone or in combination with PakK299R. (**H**) Percentage of EGFP-positive leukemic cells in mice bearing KITD814V or KITD814V in combination with PakK299R. Quantitative assessment of EGFP-positive cells ($n = 3$, $^*P < 0.05$).

its constitutive phosphorylation was observed in both KITD814V and KITD814V- and PakK299R-coexpressing cells, the activation of Pak was inhibited in cells coexpressing KITD814V and PakK299R relative to controls. Importantly, Pak repression in KITD814V-bearing cells abrogated the ligand-independent proliferation normally observed in KITD814V-bearing cells (Figure 8F). The expression of an activated version of Pak (PakT423) in Rac1/Rac2-deficient KITD814V-bearing primary HSC/Ps rescued ligand-independent growth (Supplemental Figure 8B).

We next assessed the consequence of pharmacologic inhibition of Pak on the growth of KITD814V-bearing cells using a cell-permeable allosteric inhibitor of Pak, IPA-3 (33). As seen in Figure 9A, the treatment of KITD814V-bearing P815 cells with IPA-3 resulted in the inhibition of Pak activation, and the treatment of HMC1.2 cells, P815 cells, and Kasumi-1 cells with the same inhibitor led to a dose-dependent inhibition of the growth of KITD816V- and KITD814V-bearing cells (Figure 9, B–D). Repression of the growth of oncogene KIT–bearing cells in the presence of IPA-3 was largely due to reduced survival (Figure 9E).

To directly assess the impact of Pak inhibition on KITD814V-induced MPN development, we transplanted C3H/HeJ mice with cells bearing KITD814V and PakK299R as described (27). Transplanted mice were observed for the development of MPNs and survival. Although all KITD814V-bearing mice died by day 15 after transplantation, all KITD814V- and PakK299R-coexpressing mice survived this period and showed a significant delay in disease onset (Figure 10A). To assess the changes in tissue pathology in mice bearing cells coexpressing KITD814V and PakK299R compared with those bearing only KITD814V, we sacrificed a cohort of mice on days when the KITD814V-only–bearing mice succumbed to death. As seen in Figure 10, B and C, compared with the KITD814V-bearing control mice, mice coexpressing KITD814V and PakK299R demonstrated a significant decrease in spleen weight and PB counts. In addition, these mice demonstrated a correction in splenic architecture (Figure 10E), myeloid cell infiltration in the lung (Figure 10D) and liver (Figure 10F), and lacked the lesions on lungs normally associated with KITD814V-bearing mice (Figure 10G). All of these findings were associated with a reduced percentage (as assessed by EGFP-expressing cells) of leukemic cells in the tissues of mice transplanted with cells bearing KITD814V and PakK299R (Figure 10H).

## Discussion

Rac and its downstream effector Pak are frequently overexpressed and/or hyperactive in solid cancers including breast cancer (34). In these cells, Rac and Pak have been implicated in regulating invasion and metastasis (35, 36). While substantial progress has been made in our understanding of the role of these molecules in solid cancers, how these molecules regulate oncogene-induced MPNs is poorly understood. We provide in vitro and in vivo genetic, biochemical, and pharmacologic evidence to suggest that the Vav/Rac/Pak pathway plays an essential role in regulating transformation via an oncogenic form of KIT (KITD814V) associated with MPNs and AML and for which no efficacious therapies are currently available. While gain-of-function KIT mutations localized to the juxtamembrane region associated with gastrointestinal stromal tumors (GISTs) are highly sensitive to inhibition by imatinib, KIT mutations within the second catalytic domain found in patients with AML and SM, including KITD814V, interfere with the binding of imatinib, thus rendering this mutation insensitive to imatinib inhibition (37–39). Our results suggest that inhibition of constitutively active Vav, Rac, or Pak downstream from KITD814V is a highly efficient alternative approach to treating hematologic malignancies involving this mutation.

To date, several GEFs for Rac have been identified (40, 41); however, GEFs such as those that belong to the Vav family as well as Tiam-1 have been primarily implicated in tumorigenesis (42–44). Although, the precise mechanism(s) by which these GEFs regulate cancer progression is still unclear, studies suggest that Vav GEFs are significantly more diverse in their ability to activate Rho family GTPases and can regulate the activation of Rac, Rho, and Cdc42, compared with Tiam-1 and Trio, which primarily activate Rac (17, 45–47). While it is unclear how this occurs, the presence of Src homology and cysteine-rich domains in Vav are likely to contribute to this diversity. Our findings using HSC/Ps derived from Vav1-deficient mice engineered to express KITD814V suggest an essential role for Vav1 in regulating the ligand-independent growth of oncogene-bearing cells and in activating both Rac1 and Rac2.

Our findings demonstrating the correction of myeloid cell infiltration in the lungs of mice coexpressing RacN17 or PakK299R along with KITD814V suggest that KITD814V-induced metastasis of myeloid cells in these tissues is dependent on Rac and Pak. Furthermore, our results also demonstrate that prolonged survival of KITD814V-bearing mice in the setting of RacN17 expression correlates with marked repression of Rac1, Rac2, and Pak in these cells, and loss of Rac1, Rac2, or both Rac1 and Rac2 substantially represses ligand-independent growth in these cells. These findings were also confirmed by using cells from mice bearing KITD814V in the setting of Vav1 and Rac1/Rac2 deficiency and by transplantating these cells into lethally irradiated WT recipients. Interestingly, our data implicating Rac1 and Rac2 in KITD814V-induced transformation are similar to those reported by Thomas et al. using p210BCR-ABL translocation (48). In both instances, Rac1 and Rac2 deficiency collectively shows a more prolonged survival of leukemic mice.

In addition to the genetic approaches to test the role of Rac in MPNs, we also used pharmacologic approaches to test the possibility of targeting Rac GTPases for the treatment of KITD814V-induced MPNs and AML. To this end, we first used an established Rac inhibitor, NSC23766. Previous studies have shown that NSC23766 functions by binding in the pocket of Rac1 that interacts with GEFs such as Trio and Tiam1 but not Vav (17, 49). Our results using this drug suggest that Rac1 does not greatly contribute to KITD814V-induced transformation, since we observed only a 50% reduction in the growth of both murine and human oncogene KIT–bearing cells at very high doses of NSC23766. While reasonable, an alternate explanation may involve a lack of robust involvement of Trio and Tiam1 in KITD814V-induced transformation. Therefore, in an effort to assess whether Rac GTPase could be targeted more efficiently in KIT oncogene–bearing cells, we used a newly described Rac inhibitor, EHop-016 (18). This drug is a derivative of NSC23766 and inhibits Rac 100-fold more efficiently relative to the parental compound (18). EHop-016, like NSC23766, binds to the surface groove of Rac, which is critical for interacting with GEFs. Studies have shown that EHop-016 is more potent than the parental compound in terms of its interaction with the effector domains of Rac (18). This presumably allows EHop-016 to block the activation of additional Rac GEFs in addition to those blocked by NSC23766. Our head-to-head studies comparing NSC23766 and EHop-016 show that EHop-016 is a more potent Rac inhibitor than NSC23766.

Although we have no direct evidence to suggest which additional GEFs might be inhibited by EHop-016 in oncogene KIT–bearing cells, previous studies in an MDA-MB-435 metastatic breast cancer line have shown that EHop-016 inhibits the interaction of Vav2 with Rac (18). It is therefore likely that in KITD814V-bearing HSC/Ps, EHop-016 inhibits the interaction of Vav1 with Rac1 and Rac2. We show that the treatment of oncogene-bearing cells with EHop-016 results in the inhibition of both Rac1 and Rac2. Consistent with these findings, Vav1 deficiency in oncogene-bearing cells impairs the activation of both Rac1 and Rac2 and substantially corrects the ligand-independent growth observed in WT oncogene–bearing HSC/Ps, very similar to the growth repression observed in the presence of EHop-016.

Downstream from Rac, we show that Pak plays an essential role in KITD814V-induced transformation. We used both an allosteric inhibitor of Pak, IPA-3, as well as a genetic approach to implicate Pak in KITD814V-induced transformation. Although IPA-3 selectively inhibits the activation of Pak1 (33), at higher doses it has been shown to also inhibit the activation of other isoforms including Pak2 and Pak3 (33). Our studies using a dominant-negative form of Pak (K299R) confirmed the IPA-3 findings demonstrating that Pak indeed contributes to KITD814V-induced transformation; whether other isoforms of Pak also contribute to leukemogenesis remains to be determined. As animal models deficient in the expression of Pak isoforms become available, the role of specific isoforms of Pak in transformation can be more readily and efficiently addressed in future studies. Taken together, our studies identify what we believe to be a novel pathway involving Vav/Rac and Pak in regulating nonclassical MPNs such as SM, in which activating the KIT mutation plays an essential role.

## Methods

*Cell culture*. HMC1.2 cells harboring both V560G and D816V mutations were maintained in RPMI medium supplemented with 15% heat-inactivated FBS (Hyclone; Thermo Fisher Scientific), 2% penicillin-streptomycin, and monothioglycerol at 37°C and 5% $CO_2$ (50). The murine P815 mastocytoma cell line was cultured in DMEM supplemented with 10% heat-inactivated FBS and 2% penicillin-streptomycin. 32D murine cells were cultured in RPMI with 10% FBS and 2% penicillin-streptomycin. Kasumi-1, an AML cell line, was grown in RPMI 1640 medium supplemented with 20% FBS, 1% HEPES, 1% L-glutamine, and 2% penicillin-streptomycin and were a gift from Christopher Klug (University of Alabama at Birmingham, Birmingham, Alabama, USA) (51).

*Mice, cytokines, and antibodies*. C57BL/6 mice and C3H/HeJ mice were purchased from The Jackson Laboratory. *Vav1*$^{-/-}$, *Vav2*$^{-/-}$, *Vav3*$^{-/-}$, *Rac2*$^{-/-}$, *Rac1*$^{flox/flox}$, and *Rac1*$^{flox/flox}$*Rac2*$^{-/-}$ mice have been previously described (14, 29, 52, 53). *Vav2*$^{-/-}$ and *Vav3*$^{-/-}$cells were a gift from Jose Cancelas (Cincinnati Children's Hospital Medical Center, Cincinnati, Ohio, USA). All mice used in this study were 6–12 weeks of age. Murine IL-3, murine IL-6, SCF, Flt-3 ligand (Flt-3), and thrombopoietin (TPO) were purchased from PeproTech. 2,2′-dihydroxy-1,1′-dinaphthyldisulfide (IPA-3) and NSC23766 were purchased from Tocris Bioscience. The discovery and characterization of EHop-016 have been described previously (18). The Cdc42 small–molecule inhibitor, CASIN, was a gift from Yi Zheng (Cincinnati Children's Hospital Medical Center) (54, 55).

Western blot analysis and IP experiments were performed as described previously (56). Protein expression was determined using antibodies against Rac1, Rac2, and Rac1/2/3 (Millipore), pPak, Pak, KIT, Vav1, pKIT, total ERK, pMLC, and pTyrosine (Cell Signaling Technology), pBAD (Santa Cruz Biotechnology Inc.), and β-actin (Sigma-Aldrich). Rac activity was determined by using a Rac activation kit (Millipore) according to the manufacturer's protocol and analyzed by Western blot using Rac1, Rac2, or Rac1/2/3 pan-antibody.

*Patient samples*. Cells from the BM and PB of patients with SM were analyzed for KIT mutations (57) and cultured in 100 ng human SCF in IMDM supplemented with 20% FBS and 2% penicillin-streptomycin.

*Plasmids*. pCMV6 expressing a Myc-tagged kinase-dead (K299R) Pak was a gift from Jeffrey Field (University of Pennsylvania, Philadelphia, Pennsylvania, USA) (58). Plasmids encoding RacN17 have been previously described (34). The cDNAs were subcloned into a bicistronic retroviral vector, MIEG3, upstream of the internal ribosome entry site (IRES) and the EGFP gene (59) or human CD4 gene. The pLNCX2-PAK1T423E-IRES2-EGFP plasmid has been described (60). Plasmids encoding MIEG3-RacN17 and MSCV-puro-RacV12 have been previously described (56).

*Expression of WT KIT and KITD814V receptors in 32D cells and primary HSC/Ps*. Retroviral supernatants for the transduction of 32D cells and primary BM low-density mononuclear cells (LDMNCs) were generated with a Phoenix ecotropic packaging cell line transfected with retroviral vector plasmids using a calcium phosphatase transfection kit (Invitrogen). Supernatants were collected 48 hours after transfection and filtered through 0.45-μm membranes. 32D cells were infected with 2 ml of high-titer virus supernatant in the presence of 8 μg/ml polybrene. EGFP-positive cells or human CD4-positive (hCD4-positive) cells containing the WT form of KIT or KITD814V with RacN17 or PakK299R were sorted to homogeneity and used in the experiments. BM LDMNCs were suspended in nontissue culture plates along with prestimulation media (IMDM containing 20% FBS and 2% penicillin-streptomycin supplemented with 100 ng/ml SCF, 100 ng/ml TPO, 50 ng/ml Flt-3, and 4 ng/ml IL-6) for 2 days prior to two rounds of retroviral infection using 2 ml of high-titer retroviral supernatants (WT KIT, KITD814V, pLNCX2-PAK1T423E, or MSCVpuro-RacV12) on fibronectin fragments (Retronectin; Takara). Forty-eight hours after the last infection, cells expressing WT KIT or KITD814V were sorted to homogeneity based on EGFP expression. MSCV puro cells were selected with 1 μg/ml puromycin (Sigma-Aldrich) for an additional 48 hours.

*Transplantation*. Transplantation into C3H/HeJ mice was carried out by administering a single i.v. injection of $2 \times 10^6$ 32D cells bearing WT KIT or KITD814V with or without RacN17 or PakK299R, or $1 \times 10^6$ KITD814V-bearing 32D cells cultured overnight with DMSO (vehicle), 25 μM NSC23766, or 2.5 μM EHop-016. Mice were harvested at the time of moribundity, and PB, femurs, spleen, lungs, and liver were collected for histopathological and flow cytometric analysis.

WT or *Vav1*$^{-/-}$, *Rac2*$^{-/-}$, and Mx-cre/*Rac1*$^{flox/flox}$/*Rac2*$^{-/-}$ C57BL/6 mice that were 6-to-8 weeks of age were given a single i.p. injection of 150 mg/kg of 5-fluorouracil (5-FU) (APP Pharmaceuticals). BM cells were collected 72 hours after injection from the tibia, femur, and iliac crest, and LDMNCs were prestimulated for 2 days in prestimulation media, as described above prior to transduction with retrovirus encoding WT KIT or KITD814V. After two rounds of infection as described above, cells were sorted to homogeneity, and $1 \times 10^6$ cells were counted and mixed with $1 \times 10^5$ supporting fresh splenocytes from WT C57BL/6 mice and administered i.v. by tail vein injection into lethally irradiated (1,100 cGy split dose) C57BL/6 recipient mice. We treated the recipient mice on day 14 after transplantation with two i.p. injections of 300 μg polyI:C administered at 48-hour intervals.

*Flow cytometric analysis*. Cells expressing either WT KIT or KITD814V were incubated for 30 minutes at 4°C in 10% rat serum before staining with a combination of the antibodies indicated in Figure 2A. Cells were washed two times with 0.2% BSA in PBS (Sigma-Aldrich) and analyzed by FACS (FACS and LSR; BD).

*In vitro functional assays*. Proliferation was assessed by conducting a thymidine incorporation assay. Briefly, cells were washed and starved in the presence of 0.2% BSA without serum or growth factors for 6 to 8 hours. Cells

($5 \times 10^4$) were plated in replicates of four in a 96-well plate in 200 μl complete medium either in the absence or presence of the indicated growth factors. The cells were cultured for 48 hours and subsequently pulsed with 1.0 μCi (0.037 MBq) [$^3$H] thymidine (PerkinElmer) for 6 hours and harvested using an automated 96-well cell harvester (Brandel). Thymidine incorporation was assessed as counts per minute (cpm). Apoptosis was assessed following the starvation of cells and subsequent plating in 24-well plates ($2 \times 10^5$ cells) in 0.5 ml of complete media (IMDM, 10% FBS, 2% penicillin-streptomycin) in the absence of growth factors. Apoptosis was determined following staining with an Annexin V Apoptosis Detection kit (BD Biosciences — Pharmingen) and analyzed via flow cytometry.

*Statistics*. Data are expressed as the mean ± SD unless otherwise stated. Sigma Plot 12.0 software (Systat Software Inc.) was used for statistical analysis. A *P* value less than 0.05 was considered statistically significant. The survival probability of transplanted mice cohorts was compared using Kaplan-Meier survival analysis with a log-rank test.

*Study approval*. Mice were maintained under specific pathogen-free conditions at the Indiana University Laboratory Animal Research Center, and this study was approved by the IACUC of the Indiana University School of Medicine. Samples from SM patients were collected after obtaining written informed consent as approved by the IRB of the Cleveland Clinic/Case Comprehensive Cancer Center and the IRB of the Indiana University School of Medicine and were obtained in accordance with the Declaration of Helsinki.

## Acknowledgments

We would like to thank Marilyn Wales for providing administrative support. This work was supported in part by grants from the NIH (R01HL077177, R01HL075816, and R01CA134777, to R. Kapur); F31AG040974 (to H. Martin); T32HL007910 (to A. Chatterjee); a grant from the American Cancer Society (PF13-065-01, to A. Chatterjee); and a grant from Riley Children's Foundation (to R. Kapur).

Received for publication October 24, 2012, and accepted in revised form July 11, 2013.

Address correspondence to: Reuben Kapur, Herman B Wells Center for Pediatric Research, Indiana University School of Medicine, Cancer Research Institute, 1044 W. Walnut Street, Room 168, Indianapolis, Indiana 46202, USA. Phone: 317.274.4658; Fax: 317.274.8679; E-mail: rkapur@iupui.edu.

1. Beghini A, et al. C-kit mutations in core binding factor leukemias. *Blood*. 2000;95(2):726–727.
2. Hirota S, et al. Gain-of-function mutations of c-kit in human gastrointestinal stromal tumors. *Science*. 1998;279(5350):577–580.
3. Nagata H, et al. Identification of a point mutation in the catalytic domain of the protooncogene c-kit in peripheral blood mononuclear cells of patients who have mastocytosis with an associated hematologic disorder. *Proc Natl Acad Sci U S A*. 1995; 92(23):10560–10564.
4. Gerbaulet A, et al. Mast cell hyperplasia, B-cell malignancy, and intestinal inflammation in mice with conditional expression of a constitutively active kit. *Blood*. 2011;117(6):2012–2021.
5. Kitayama H, et al. Constitutively activating mutations of c-kit receptor tyrosine kinase confer factor-independent growth and tumorigenicity of factor-dependent hematopoietic cell lines. *Blood*. 1995; 85(3):790–798.
6. Piao X, Bernstein A. A point mutation in the catalytic domain of c-kit induces growth factor independence, tumorigenicity, and differentiation of mast cells. *Blood*. 1996;87(8):3117–3123.
7. Tsujimura T, et al. Ligand-independent activation of c-kit receptor tyrosine kinase in a murine mastocytoma cell line P-815 generated by a point mutation. *Blood*. 1994;83(9):2619–2626.
8. Ustun C, DeRemer DL, Akin C. Tyrosine kinase inhibitors in the treatment of systemic mastocytosis. *Leuk Res*. 2011;35(9):1143–1152.
9. Pardanani A. Systemic mastocytosis in adults: 2011 update on diagnosis, risk stratification, and management. *Am J Hematol*. 2011;86(4):362–371.
10. Munugalavadla V, Sims EC, Chan RJ, Lenz SD, Kapur R. Requirement for p85alpha regulatory subunit of class IA PI3K in myeloproliferative disease driven by an activation loop mutant of KIT. *Exp Hematol*. 2008;36(3):301–308.
11. Ma P, Mali RS, Martin H, Ramdas B, Sims E, Kapur R. Role of intracellular tyrosines in activating KIT-induced myeloproliferative disease. *Leukemia*. 2012; 26(7):1499–1506.
12. Katzav S, Martin-Zanca D, Barbacid M. vav, a novel human oncogene derived from a locus ubiquitously expressed in hematopoietic cells. *EMBO J*. 1989; 8(8):2283–2290.
13. Katzav S. Vav1: a hematopoietic signal transduction molecule involved in human malignancies. *Int J Biochem Cell Biol*. 2009;41(6):1245–1248.
14. Fujikawa K, et al. Vav1/2/3-null mice define an essential role for Vav family proteins in lymphocyte development and activation but a differential requirement in MAPK signaling in T and B cells. *J Exp Med*. 2003;198(10):1595–1608.
15. Gakidis MA, et al. Vav GEFs are required for beta2 integrin-dependent functions of neutrophils. *J Cell Biol*. 2004;166(2):273–282.
16. Williams DA, Zheng Y, Cancelas JA. Rho GTPases and regulation of hematopoietic stem cell localization. *Methods Enzymol*. 2008;439:365–393.
17. Gao Y, Dickerson JB, Guo F, Zheng J, Zheng Y. Rational design and characterization of a Rac GTPase-specific small molecule inhibitor. *Proc Natl Acad Sci U S A*. 2004;101(20):7618–7623.
18. Montalvo-Ortiz BL, et al. Characterization of EHop-016, novel small molecule inhibitor of Rac GTPase. *J Biol Chem*. 2012;287(16):13228–13238.
19. Arias-Romero LE, Chernoff J. A tale of two Paks. *Biol Cell*. 2008;100(2):97–108.
20. Eswaran J, Soundararajan M, Knapp S. Targeting group II PAKs in cancer and metastasis. *Cancer Metastasis Rev*. 2009;28(1–2):209–217.
21. Adam L, Vadlamudi R, Kondapaka SB, Chernoff J, Mendelsohn J, Kumar R. Heregulin regulates cytoskeletal reorganization and cell migration through the p21-activated kinase-1 via phosphatidylinositol-3 kinase. *J Biol Chem*. 1998;273(43):28238–28246.
22. Delorme V, et al. Cofilin activity downstream of Pak1 regulates cell protrusion efficiency by organizing lamellipodium and lamella actin networks. *Dev Cell*. 2007;13(5):646–662.
23. Sells MA, Knaus UG, Bagrodia S, Ambrose DM, Bokoch GM, Chernoff J. Human p21-activated kinase (Pak1) regulates actin organization in mammalian cells. *Curr Biol*. 1997;7(3):202–210.
24. Balasenthil S, et al. p21-activated kinase-1 signaling mediates cyclin D1 expression in mammary epithelial and cancer cells. *J Biol Chem*. 2004;279(2):1422–1428.
25. Ito M, et al. P21-activated kinase 1: a new molecular marker for intravesical recurrence after transurethral resection of bladder cancer. *J Urol*. 2007; 178(3 pt 1):1073–1079.
26. Schraml P, et al. Combined array comparative genomic hybridization and tissue microarray analysis suggest PAK1 at 11q13.5-q14 as a critical oncogene target in ovarian carcinoma. *Am J Pathol*. 2003; 163(3):985–992.
27. Mali RS, et al. Rho kinase regulates the survival and transformation of cells bearing oncogenic forms of KIT, FLT3, and BCR-ABL. *Cancer Cell*. 2011; 20(3):357–369.
28. Oberley MJ, Wang DS, Yang DT. Vav1 in hematologic neoplasms, a mini review. *Am J Blood Res*. 2012; 2(1):1–8.
29. Gu Y, et al. Hematopoietic cell regulation by Rac1 and Rac2 guanosine triphosphatases. *Science*. 2003; 302(5644):445–449.
30. Chan PM, Manser E. PAKs in human disease. *Prog Mol Biol Transl Sci*. 2012;106:171–187.
31. Ong CC, et al. p21-activated kinase 1: PAK'ed with potential. *Oncotarget*. 2011;2(6):491–496.
32. Ong CC, et al. Targeting p21-activated kinase 1 (PAK1) to induce apoptosis of tumor cells. *Proc Natl Acad Sci U S A*. 2011;108(17):7177–7182.
33. Deacon SW, et al. An isoform-selective, small-molecule inhibitor targets the autoregulatory mechanism of p21-activated kinase. *Chem Biol*. 2008; 15(4):322–331.
34. Schnelzer A, et al. Rac1 in human breast cancer: overexpression, mutation analysis, and characterization of a new isoform, Rac1b. *Oncogene*. 2000; 19(26):3013–3020.
35. Chan AY, et al. Roles of the Rac1 and Rac3 GTPases in human tumor cell invasion. *Oncogene*. 2005; 24(53):7821–7829.
36. Burbelo P, Wellstein A, Pestell RG. Altered Rho GTPase signaling pathways in breast cancer cells. *Breast Cancer Res Treat*. 2004;84(1):43–48.
37. Singer S, et al. Prognostic value of KIT mutation type, mitotic activity, and histologic subtype in gastrointestinal stromal tumors. *J Clin Oncol*. 2002; 20(18):3898–3905.
38. Frost MJ, Ferrao PT, Hughes TP, Ashman LK. Juxtamembrane mutant V560GKit is more sensitive to Imatinib (STI571) compared with wild-type c-kit whereas the kinase domain mutant D816VKit is resistant. *Mol Cancer Ther*. 2002;1(12):1115–1124.
39. Ma Y, et al. The c-KIT mutation causing human mastocytosis is resistant to STI571 and other KIT kinase inhibitors; kinases with enzymatic site mutations show different inhibitor sensitivity profiles than wild-type kinases and those with regulatory-type mutations. *Blood*. 2002;99(5):1741–1744.
40. Rossman KL, Der CJ, Sondek J. GEF means go: turning on RHO GTPases with guanine nucleotide-exchange factors. *Nat Rev Mol Cell Biol*. 2005; 6(2):167–180.
41. Schmidt A, Hall A. Guanine nucleotide exchange factors for Rho GTPases: turning on the switch. *Genes Dev*. 2002;16(13):1587–1609.
42. Palmby TR, Abe K, Karnoub AE, Der CJ. Vav transformation requires activation of multiple GTPases

and regulation of gene expression. *Mol Cancer Res*. 2004;2(12):702–711.
43. Miller SL, DeMaria JE, Freier DO, Riegel AM, Clevenger CV. Novel association of Vav2 and Nek3 modulates signaling through the human prolactin receptor. *Mol Endocrinol*. 2005;19(4):939–949.
44. Minard ME, Kim LS, Price JE, Gallick GE. The role of the guanine nucleotide exchange factor Tiam1 in cellular migration, invasion, adhesion and tumor progression. *Breast Cancer Res Treat*. 2004;84(1):21–32.
45. Liu BP, Burridge K. Vav2 activates Rac1, Cdc42, and RhoA downstream from growth factor receptors but not beta1 integrins. *Mol Cell Biol*. 2000; 20(19):7160–7169.
46. Chrencik JE, et al. Structural basis of guanine nucleotide exchange mediated by the T-cell essential Vav1. *J Mol Biol*. 2008;380(5):828–843.
47. Abe K, et al. Vav2 is an activator of Cdc42, Rac1, and RhoA. *J Biol Chem*. 2000;275(14):10141–10149.
48. Thomas EK, et al. Rac guanosine triphosphatases represent integrating molecular therapeutic targets for BCR-ABL-induced myeloproliferative disease. *Cancer Cell*. 2007;12(5):467–478.
49. Binker MG, Binker-Cosen AA, Gaisano HY, Cosen-Binker LI. Inhibition of Rac1 decreases the severity of pancreatitis and pancreatitis-associated lung injury in mice. *Exp Physiol*. 2008;93(10):1091–1103.
50. Furitsu T, et al. Identification of mutations in the coding sequence of the proto-oncogene c-kit in a human mast cell leukemia cell line causing ligand-independent activation of c-kit product. *J Clin Invest*. 1993;92(4):1736–1744.
51. Asou H, Tashiro S, Hamamoto K, Otsuji A, Kita K, Kamada N. Establishment of a human acute myeloid leukemia cell line (Kasumi-1) with 8;21 chromosome translocation. *Blood*. 1991; 77(9):2031–2036.
52. Roberts AW, et al. Deficiency of the hematopoietic cell-specific Rho family GTPase Rac2 is characterized by abnormalities in neutrophil function and host defense. *Immunity*. 1999;10(2):183–196.
53. Turner M, et al. A requirement for the Rho-family GTP exchange factor Vav in positive and negative selection of thymocytes. *Immunity*. 1997; 7(4):451–460.
54. Florian MC, et al. Cdc42 activity regulates hematopoietic stem cell aging and rejuvenation. *Cell Stem Cell*. 2012;10(5):520–530.
55. Peterson JR, Lebensohn AM, Pelish HE, Kirschner MW. Biochemical suppression of small-molecule inhibitors: a strategy to identify inhibitor targets and signaling pathway components. *Chem Biol*. 2006;13(4):443–452.
56. Tan BL, et al. Genetic evidence for convergence of c-Kit- and alpha4 integrin-mediated signals on class IA PI-3kinase and the Rac pathway in regulating integrin-directed migration in mast cells. *Blood*. 2003;101(12):4725–4732.
57. Traina F, et al. Single nucleotide polymorphism array lesions, TET2, DNMT3A, ASXL1 and CBL mutations are present in systemic mastocytosis. *PLoS One*. 2012;7(8):e43090.
58. Tang Y, Zhou H, Chen A, Pittman RN, Field J. The Akt proto-oncogene links Ras to Pak and cell survival signals. *J Biol Chem*. 2000;275(13):9106–9109.
59. Williams DA, et al. Dominant negative mutation of the hematopoietic-specific Rho GTPase, Rac2, is associated with a human phagocyte immunodeficiency. *Blood*. 2000;96(5):1646–1654.
60. Li Q, Mullins SR, Sloane BF, Mattingly RR. p21-Activated kinase 1 coordinates aberrant cell survival and pericellular proteolysis in a three-dimensional culture model for premalignant progression of human breast cancer. *Neoplasia*. 2008; 10(4):314–329.